Natural or synthetic? Simultaneous Raman/luminescence hyperspectral microimaging for the fast distinction of ultramarine pigments

González-Cabrera, M., Arjonilla, P., Domínguez-Vidal, A., Ayora-Cañada. M.J.*

Department of Physical and Analytical Chemistry, Universidad de Jaén, Campus Las Lagunillas, s/n, 23071, Jaén, Spain

*Corresponding author. E-mail address: mjayora@ujaen.es

Abstract

Genuine ultramarine has been one of the most precious blue pigments employed since ancient times. It used to be obtained by crushing and grinding the lapis lazuli rock and selectively extracting the blue mineral lazurite. Since 1828, when it was produced the synthetic version, the use of this much less expensive material became widespread and synthetic ultramarine blue replaced the natural one in painting palettes. The distinction between natural and synthetic ultramarine is, therefore, an important goal in authentication issues. Here, we present a hyperspectral microRaman imaging analysis, complemented with the characterization of ultramarine pigment samples in terms of colour, elemental composition and identification of crystalline phases by means of fiber optics reflection spectroscopy (FORS), X-Ray Fluorescence (XRF) and X-Ray diffraction (XRD), respectively. We show that a characteristic luminescence signature, easily detected in the course of standard Raman spectroscopic analysis using 785 nm as excitation, is indicative of the natural origin of the ultramarine blue pigments. Furthermore, simultaneous Raman/luminescence hyperspectral microimages allow the distinction between natural pigments of different quality thanks to the different intensity and spatial distribution of the lazurite characteristic band at 548 cm^{-1} and those of the luminescent impurities in the region between 1200 and 2000 cm^{-1}. The establishement of a range of quality between different samples of lapis lazuli was also attempted taking into account the variations in the intensity of the Raman bands located at 548 cm^{-1} and 1286 cm^{-1}. Finally, the feasibility of using the simultaneous Raman/luminescence features for authentication of ultramarine blue in a real historical context, even with non-invasive investigations, is illustrated with examples of different types of blue decorations from several halls of the Alhambra monumental ensemble, in Granada.

Keywords: hyperspectral imaging, Raman microspectroscopy, lazurite, ultramarine, lapis lazuli, luminescence.

1.- Introduction

Ultramarine was a very expensive and precious blue pigment extensively used in Europe throughout the 14th and 15th centuries in mediaeval paintings and frescoes. This precious pigment took on an iconographic value and it was reserved for the robes of only the most prominent figures, such as Christ and the Virgin Mary in religious scenes. The first known use of lapis lazuli pigment dates back to the 6th and 7th centuries CE, in paintings of cave temples in Afghanistan [1]. The oldest western paintings where lapis lazuli has been found are in the church of San Saba (Rome), dating to the first half of the 8th century CE [2]. The mineral responsible for the blue colour of lapis lazuli is lazurite ($Na_8Al_6Si_6O_{24}S_n$), a member of the aluminosilicate group, with the same structure as sodalite ($Na_8Al_6Si_6O_{24}Cl_2$) [3]. It comprises interconnected AlO_4 and SiO_4 tetrahedra joined to form a three-dimensional framework with anions and cations located inside the large central cavities, commonly designated as β-cages [4][5][6]. Lazurite's colour is attributed to sulfur polyanions trapped in the β-cages, being the trisulfur radical ($S_3^{-\cdot}$) mainly responsible for the blue colour. Contributions from disulfur ($S_2^{-\cdot}$) and tetrasulfur ($S_4^{-\cdot}$) radicals can shift the colour towards yellow or red, respectively. Thus, the proportion of different sulfur species is regarded as one of the decisive factors influencing the final aspect of the pigment [7]. The most famous traditional method to purify lazurite as reported in Cennino Cennini's Il Libro dell'Arte [8], is a lengthy extraction process. Natural lazurite occurs in association with other minerals like calcite ($CaCO_3$) [9], pyrite (FeS_2) [10], diopside ($CaMgSi_2O_6$) [9][11], wollastonite ($CaSiO_3$) [10], forsterite (Mg_2SiO_4) [10], phlogopite ($K(Mg,Fe,Mn)_3Si_3AlO_{16}(F(OH)_2$) [9], muscovite ($KAl_2(AlSi_3O_{10})(OH)_2$) [10], and other sodalite group members such as nosean ($Na_8Si_6Al_6O_{24}(SO_4)\cdot H_2O$) [10][11] and haüyne ($Na_3CaSi_3Al_3O_{12}(SO_4)$) [10][12] depending on the geographical origin of the rock. Thus, the purification process involved the mixing of finely ground lapis lazuli with pine rosin, gum mastic, and beeswax to form the so-called *pastello*. The *pastello* was then stored and massaged in a warm solution of plant ashes, which preferentially separated the blue lazurite particles. Repeated several times, this process produced several grades of pigment. The first grade possesses a deep blue hue whereas the last and crudest grade has a pale-blue hue and is typically called ultramarine ash [13].
In 1828, a synthetic version of the ultramarine blue pigment was first obtained by means of a chemical process involving both calcination and oxidation steps [14]. Owning a similar composition to lazurite, the use of its synthetic analogue, $Na_{6-10}Al_6Si_6O_{24}S_{2-4}$, quickly spread across Europe during the 19th century, replacing the natural one in many of its applications, since it was cheaper and easier to produce but maintaining the appreciated bright blue aspect. Thenceforth, the identification and discrimination between natural and the synthetic ultramarine pigments is relevant

to the analysis of works of art. The occurrence of anachronistic modern pigments like synthetic ultramarine blue in historic paintings could be particularly interesting in authentication issues and/or for the detection of unknown subsequent restoration interventions. Multitechnique approaches have been found useful in order to identify accessory minerals and impurities present only in natural pigments and absent in artificial ones. Thus, different combinations of techniques including pulsed laser-induced breakdown spectroscopy (LIBS), scanning electron microscopy-energy dispersive X-ray spectroscopy (SEM/EDX) and Raman microspectroscopy have been described [15][16][17]. Nevertheless, the use of a unique analytical technique to distinguish synthetic from natural pigments and among different quality grades in a fast, reliable and even in a non-invasive manner is still an analytical challenge. Miliani et al. [18] proposed the use of a distinctive band in the FT-IR spectrum of natural Afghan lapis lazuli which was first observed by researchers at the Getty Conservation Institute (GCI) [19]. This band, located at around 2340 cm^{-1}, was absent in the spectra of the synthetic versions and in Chilean natural ultramarine. They attributed the band to entrapped carbon dioxide and proposed its use as a geographical marker. Smith and Klinshaw [20] corroborated the assignment to trapped CO_2 in the β-cage of lazurite. Nevertheless, they proved that its absence cannot be taken necessarily as a sign of synthetic ultramarine since poor quality lapis lazuli samples and highly processed natural pigment samples did not show this band. Thus, the possibility of using this spectral feature as a geographic marker is questioned [20]. The use of fiber optics reflectance spectroscopy (FORS) has been also recently explored with the purpose of distinguishing between different quality ultramarine pigments since UV-visible reflectance spectra exhibit certain differences [21]. In this case and, in combination with some unsupervised chemometric analysis, the differentiation between natural and synthetic ultramarine blue was possible, showing certain difficulties when white pigments were added to the blue ones. Raman spectroscopy has also been suggested but only subtle differences between the spectra of synthetic ultramarine blue and lazurite from lapis lazuli rocks of different geographical sources were found. Thus, their differentiation required very high spectral quality, which involved long acquisition times and very accurate calibration of the spectrometer [22]. In this work, we further explore the possibilities of this technique by exploiting the additional information provided by laser-induced luminescence of accessory minerals that occurs when recording the Raman spectra of natural ultramarine blue pigments at certain excitation wavelengths. In particular, the use of hyperspectral micro-imaging to simultaneously gather Raman and luminescence signals to map sample heterogeneities will be explored. This methodology is in a constantly growing state, due to its ability to provide not only spectral information about complex samples but also the spatial distribution of any of the components present in the registered zone of interest [23][24].

2.- Materials and methods

2.1 Pigment samples

Six ultramarine blue pigments in the form of powders were purchased from Kremer Pigmente GmbH & Co. KG (Germany). The codes and descriptions are included in Table 1 where it can be seen that four natural samples of different quality, as well as two synthetic ones, were considered. They had been prepared from lapis lazuli rock according to traditional procedures as stated by the supplier.

Table 1. Natural and synthetic ultramarine blue pigments employed in this study.

Sample code	Kremer name	Kremer reference	Description
NU-1	Purest *lapis lazuli*	10530.12010.315	Clear, distinct blue.
NU-2	*Lapis lazuli*, good quality	10520.12010.104	Natural ultramarine, good quality
NU-3	*Lapis lazuli*, medium quality	10510.12010.104	Natural ultramarine, medium quality
UA	Ultramarine ash	10580.12050.104	By-product of purest *Lapislazuli*
SU-1	Ultramarine blue, dark	45010.12100.136	Synthetic mineral pigment
SU-2	Ultramarine blue, greenish extra	45030.12100.136	Synthetic mineral pigment

2.2. Historical blue decorations

The decorative revetments of the Alhambra monumental ensemble (Granada, Spain) have been investigated by our research group during the last years [25][26][27][28][29]. These studies have paid special attention to the materials employed in the Nasrid original decorations as well as to the redecorations and they were performed in cooperation with the conservation experts of the Alhambra Council. The blue colour is widely used in the decoration of the Alhambra [30][31], thus we consider for this study *in situ* measurements of the blue decorations in different spaces and revetments (plasterwork, marble capitals and wooden ceilings) as well as two small fragments of plasterwork from the Hall of the Kings. These fragments, from vaults V4 and V6, were detached during a conservation intervention carried out to consolidate the stalactite vaults of this space [26].

2.3. Instrumentation

Raman spectra were recorded by using an XploRA-Plus full confocal Raman microscope, equipped with two lasers for excitation: 532 nm (25mW) and 785 nm (100 mW) and an electron-multiplying CCD (EMCCD) detector from Horiba (Kyoto, Japan). Single measurement conditions were optimized for each sample, always considering their peculiarities to achieve a good signal-to-noise ratio in the spectra and maintaining the laser power lower than 10 mW to prevent any sort of damage.

Hyperspectral point to point scanning imaging method was used, in which a single spectrum of a small pixel of the desired area is recorded at a time [24]. For the mapping analysis, 10X objective was used, resulting in a spot size of ~4 μm and a power density on samples of 0,625 mW/μm^2. The pixel size was established to 10 μm x 10 μm and total lateral area scanned was set to 140 μm x 140 μm. The number of scans and acquisition time were set to 1 and 5 seconds per scan. Each mapping was recorded reaching a minimum of 180 spectra, fixing the same area of each sample for the analysis with the two excitation wavelengths, with an average time consumption of 15 minutes per map. Initial data pretreatment was performed by using LabSpec6 (Spectroscopy Suite) commercial software from Horiba. Spectra were firstly baseline corrected and normalized by area. ImageLab software (Epina GmbH, Austria) was used to calculate distribution maps in false colour taking areas with baseline points from 520 to 565 cm^{-1} for the band located at 548 cm^{-1} and from 1260 to 1355 cm^{-1} for the one at 1286 cm^{-1}. A sort of ratio of the intensities of the bands at 1286 cm^{-1} (I1) and 548 cm^{-1} (I2) was also calculated. This ratio is mathematically calculated as the logarithm of the ratio of two peak intensities at two different wavelengths weighted by the intensity of the second peak. That is:

$$Ratio = I2\ ln\frac{(I1)}{(I2)}$$

For quantitative estimations, black/white maps were created after a thresholding operation. A threshold of 1.5 out of the maximum intensity of 10 was set allowing the distinction of a band from the noise. The threshold value was estimated considering the average signal to noise ratio in regions without clear spectral features after normalization and multiplying it by a factor of 3. Those values lying under this threshold were converted to black and all pixels with values above the threshold converted to white. In this way, the percentage of pixels above the threshold was calculated.

Historical blue decorations from the Alhambra monumental ensemble (Granada, Spain) were investigated *in situ* using a portable Raman microspectrometer innoRam (B&W TEK Inc., Newark, USA). It is equipped with a CCD detector thermoelectrically cooled to −20°C and a 785 nm excitation laser (300 mW). The spectral range was defined to 65–2000 cm^{-1}.

Reflectance measurements in the range from 370 nm to 1000 nm were carried out with a compact Bluewave-Vis spectrometer (StellarNet) equipped with a charge-coupled detector and employing a tungsten krypton lamp. The sample is illuminated over a surface area of ca. 4 mm^2 at a distance of 15 mm. A 45º/45º back scattering configuration was used. The spectrum of a 50 mm Halon reflectance standard (STN-RS50) was set as a reference. Colorimetric parameters in the CIELAB space, being L* for the lightness, a* from green (−) to red (+), and b* from blue (−) to yellow (+) [32], were then calculated from the reflectance spectra.

A Niton XL3t GOLDD+ X-ray fluorescence analyser was used. It is a handheld instrument equipped with a sensitive silicon drift detector, an X-ray tube (silver anode, 6-50 kV, 0-200 μA) and a CCD camera to visualize the sample. Samples were placed on circular Mylar® films (polypropylene 4 μm thick) in the shielded test stand, which provides a safe platform for the analysis of small and irregularly shaped samples. The small spot option, which reduced the area of measurement to 3 mm in diameter by means of a beam collimator, was used. The measurement mode "mining" performed four scans with filters optimized for the different elements. Total measurement time consuming for each sample was of 120 seconds. An in-built factory calibration based on fundamental parameters specifically indicated to measure elements in minerals in concentrations higher than 1%, provided a semi-quantitative estimation. Only the elements with concentrations above the LOD were considered.

X-ray powder diffractograms were acquired using an Empyrean X-ray Diffractometer from Malvern PANalytical Ltd (United Kingdom). Measurements were carried out by using Cu-Kα radiation (45kV, 40mA) and a PIXcel 3D detector, in the angular range of 5°-80°(2Θ) with a step of 0.01°(λ=1,540593). For the data analysis, diffractograms were baseline corrected and profile fitted. Phase identification was performed by comparison to database standard X-ray powder patterns using HighScore software. The Rietveld analysis method was used for quantification [33]. Refinement factors as the weighted residual profile (WRP) and the goodness of fit (GOF) were used for the monitoring of the convergence of the refinement.

3.- Results

3.1 Pigments characterization: colour and elemental composition.

An initial characterization of the commercial pigments samples was achieved by FORS and XRF before the study with Raman spectroscopy. Figure 1a shows the reflectance spectra obtained for the different samples. All of them present a broad band of minimum reflectance at around 600 nm. This band, attributed to the S_3^- radical trapped in the structural sodalite cages of lazurite [34], is directly related to the blue nuance of lapis lazuli. It displays different intensities depending on the type and quality of the pigment samples. As can be seen, synthetic ultramarine samples show the most intense absorption with minimum reflectance values, whereas in natural pigments there is a notable increase of reflectance. There are also slight differences in the position of the maximum reflectance band near 450 nm. This was reported as an indicator for the distinction of synthetic ultramarine pigments that present a maximum reflectance located at 450 nm compared with the slightly shifted position (455-458 nm) for the natural ones. However, this movement can be induced by several factors, including the mixing of the blue pigment with white material as already pointed out by Aceto *et al*

[21]. In fact, here, as illustrated by the differences between the samples of the natural pigments with different quality, this shift cannot be used as a clear indicator of the origin of the pigment.

An additional band, only observed in the case of the purest ultramarine sample (NU-1), with a reflectance minimum at 401 nm is observed. This band has been traditionally attributed to the S_2^- anion, which provides a certain yellow hue [35]; however other authors reported that HS_3^- species can contribute to the absorption of radiation around 400 nm [36]. Finally, some differences are also apparent in the shape of the spectra in the near-infrared region but they neither provide clear differentiation between natural and artificial samples. In order to illustrate the differences in colour observed among the samples, a graph including the CIELAB parameters a* and b* for each of them is shown in Figure 1b. As it is observed, synthetic samples are the bluest ones, being the SU2 marginally greener than SU1, which is in agreement with the description of the manufacturer. On the other hand, the blue hue is less pronounced in the natural pigments, and it decreases in concordance with the quality of the pigment indicated by the manufacturer. The ultramarine ash pigment (UA), obtained in the last extraction from the lapis lazuli rock, is very close to the centre since it contains a high proportion of colourless material, so it could barely be described as a blue pigment. Regarding the parameter L*, which gives information about the lightness exhibited by the pigments, the natural pigments exhibited higher values than the synthetic ones. Considering only the natural samples, the lower the quality, the lighter the pigment.

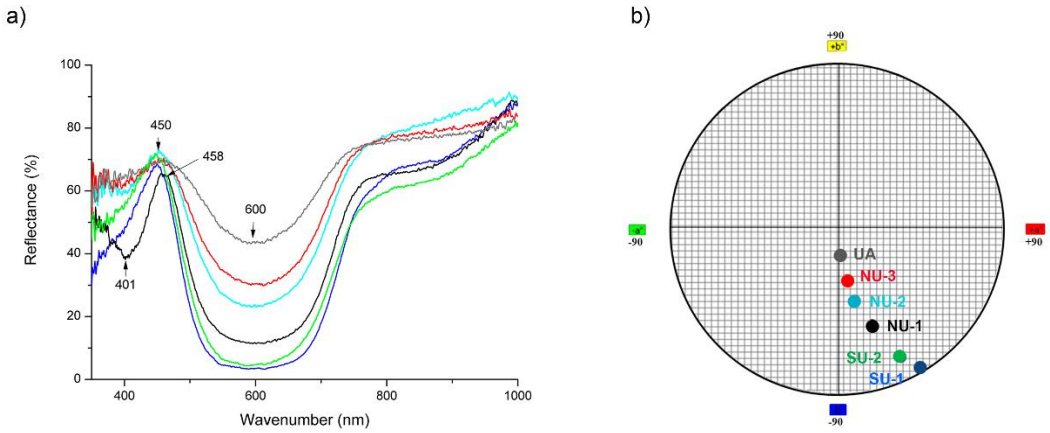

Figure 1. Colour characterization of the pigments: (a) Reflectance spectra and (b) CIELAB space including colour parameters a* and b*. Colour code for both graphs (●) NU-1, (●) NU-2, (●) NU-3, (●) UA, (●) SU-1 and (●) SU-2.

These colour differences are related to differences in the chemical composition of the pigments as shown by X-ray fluorescence. In Figure 2 the concentration of the main elements in the pigments is compared.

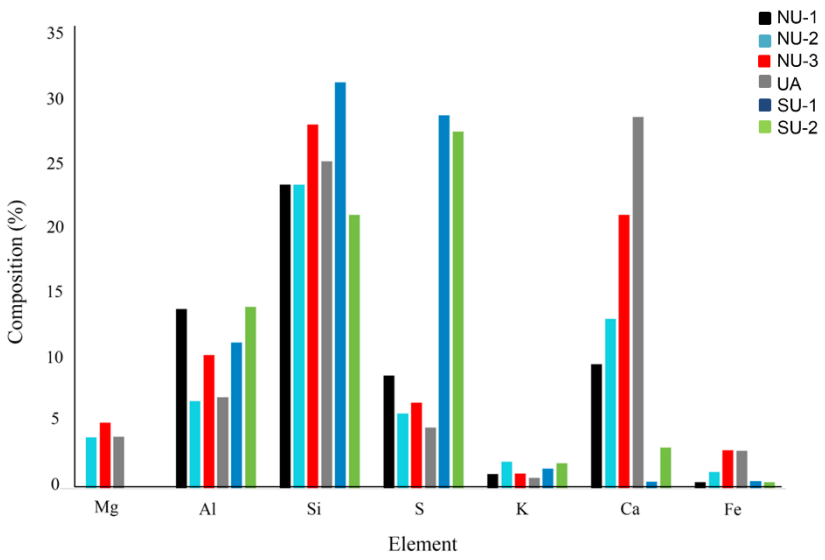

Figure 2. Relative elemental composition (%) of the different pigment samples obtained by X-ray fluorescence.

The major differences are observed for S, with significantly higher concentration for the synthetic samples. Noticeable differences are also found in Ca and Mg contents, being the latter below the limit of detection in the synthetic pigments and also in the purest ultramarine. The Ca content is also lower for the synthetic samples, and in fact, the content in natural samples is clearly related to the quality. The lower the quality, the higher the Ca content. This can be due to the presence of calcium-rich accessory minerals other than lazurite in the lower quality pigments. No clear differences were found for Si and Al contents. This could be explained because the most commonly employed synthesis methods of ultramarine blue involved the use of natural sources quite rich in Al and Si like kaolin, ($Al_2Si_2O_5(OH)_4$) [37], different kinds of zeolites [38], sodalite ($Na_8Al_6Si_6O_{24}Cl_2$) and other aluminosilicate compounds [4] as raw materials.

3.2 Raman Microspectroscopy

Single point Raman spectra and hyperspectral microimages of natural and synthetic pigments were recorded in order to characterize not only the mean spectral features of the samples but also their spatial distribution. Typical Raman spectra using two different excitation sources (532 and 785 nm) of high quality natural and synthetic ultramarine are shown in Figure 3. All of them exhibit the characteristic Raman fingerprint of lazurite, which is dominated by the band located at 548 cm^{-1} and attributed to the symmetric stretching vibration of S_3^- radicals.

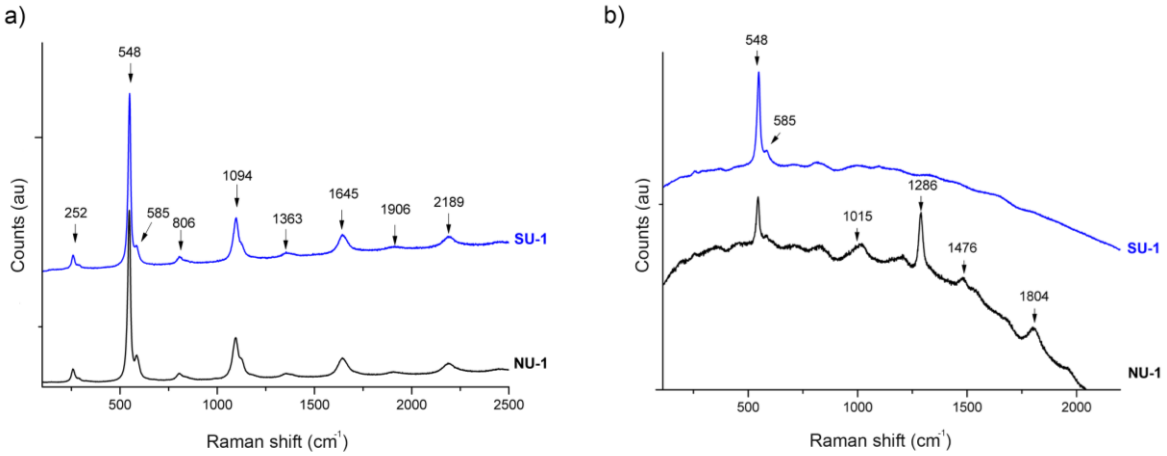

Figure 3. Raman spectra of SU-1 (blue) and NU-1 (black) samples acquired when using a (a) 532 nm and (b) 785 nm laser excitation.

Furthermore, the resonance enhancement of the Raman spectrum when using green or red radiation (between 510 and 647 nm) for excitation [39] allows for the observation of additional bands when 532 nm is used as excitation source. This is the case of the corresponding band of the bending vibration of S_3^- at 252 cm^{-1} and the overtones at 1094 cm^{-1} and 1645 cm^{-1} (first and second overtones of the S_3^- stretching mode, respectively). An additional shoulder appears at 585 cm^{-1}, commonly associated with either the symmetric stretching of S_2^- radical [40] or with the asymmetric stretching of S_3^- [41], being more visible in the samples of natural pigments.

The similarity between the spectra of the natural and synthetic samples recorded at 532 nm contrasts with those obtained when using excitation at 785 nm (Figure 3b). Both spectra exhibit a broad fluorescence background. However, in the case of the natural pigment, several bands appear in the range between 1000 and 2000 cm^{-1}, being the most intense located at 1286, 1476 and 1804 cm^{-1}. Similar features, with slight differences in band positions, have already been reported to occur only for genuine lapis lazuli rock or for genuine natural pigments [42][43][25]. However, little attention has been paid to fully exploit their potential for discrimination between natural and synthetic pigments and to the investigation of their origin with the exception of the work performed by Schmidt et al [10]. They demonstrated that the strong features observed in Raman spectra of lapis lazuli rocks and natural pigments above 1100 cm^{-1} were not the result of Raman scattering as they did not appear in the anti-Stokes region. They attributed these features to fluorescence emission bands resulting from an electronic mechanism activated by exposure of associated minerals to 785 nm radiation, suggesting that they could be related to the presence of diopside impurities containing some transition metals. Although the latter hypothesis was not definitely proved, these luminescence patterns were also found to be strongly dependent on the geographical origin of the natural rock [26].

Therefore, the luminescence features registered simultaneously with the Raman response when using excitation at 785 nm can enable a fast and non-destructive differentiation between natural and synthetic pigments. Here, we further investigate the characteristics of this luminescence emission using hyperspectral microimages to characterize the spatial distribution of both Raman and luminescence features in natural ultramarine blue taking into account samples of synthetic and natural pigments of different quality.

First, the hyperspectral images of natural (pure sample) and synthetic samples were compared. As can be seen in Figure 4, the lazurite characteristic band at 548 cm^{-1} is almost homogeneously distributed in the synthetic ultramarine sample. It should be noted that, in this case, the bright areas observed in the visible image are just artefacts due to the reflection of light. In the case of the natural ultramarine, blue and colourless areas can be observed in the visible image. In the false colour image, the lazurite band shows an uneven distribution, being much more intense in those areas corresponding to the blue areas of the visible image. To visualize the luminescence effect, the false-colour distribution maps of the ratio between the intensities of the luminescence band at 1286 cm^{-1} (I1) and the lazurite Raman band at 548 cm^{-1} (I2) are presented for natural and synthetic pigments using both excitation sources (532 and 785 nm). According to the mathematical definition of this ratio (see Materials and Methods), the map shows negative values when the I2 < I1 and the bigger is the difference between both, more negative is the value. The luminescence band is absent with the 532 nm laser wavelength, which is in concordance with the individual spectra described above. However, with the 785 nm laser excitation, a distribution of higher intensity in the white areas is detected in the natural sample, whilst it barely appears in the synthetic one.

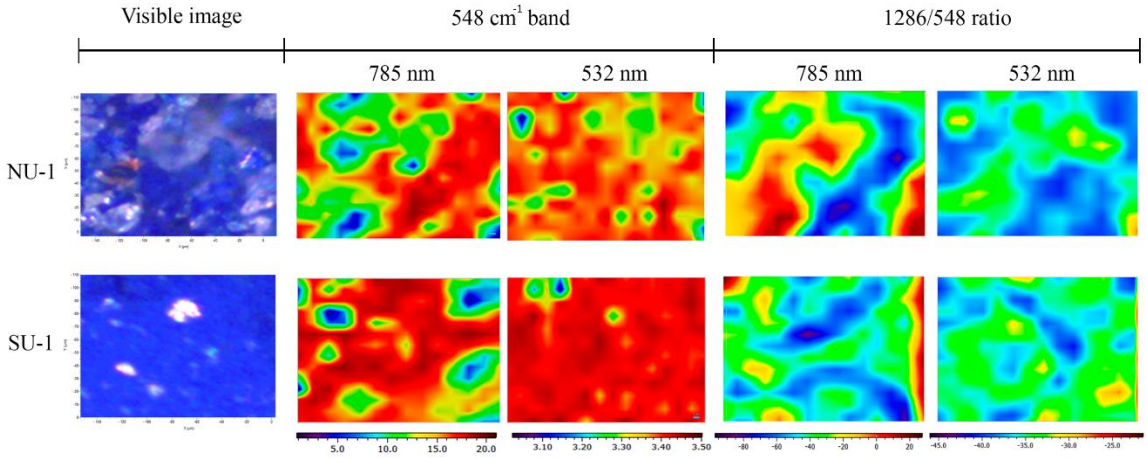

Figure 4. Visible images of NU-1 and SU-1 samples and corresponding distribution maps of the area of the band at 548 cm^{-1} and the ratio 1286/548 recorded with both excitation wavelengths.

Furthermore, the possibility of distinguishing between several natural ultramarine pigments of different qualities has also been explored in this work. Hyperspectral Raman/luminescence micro-

images obtained with 785 nm laser for excitation are shown in Figure 5. It is clear from the distribution maps that the intensity of the lazurite band at 548 cm^{-1} decreases with decreasing quality. Thus, it can be associated with the intense blue particles that are observed in the visible images (less abundant in the samples of lower quality). On the contrary, the intensity of the luminescence band at 1286 cm^{-1} increases in the samples of lower quality, being particularly intense in NU-3 and UA samples. According to Schmidt et al [10], the monoclinic pyroxene mineral diopside ($CaMgSi_2O_6$) could be the cause of the appearance of luminescence bands in the Raman spectra of natural ultramarine pigments.

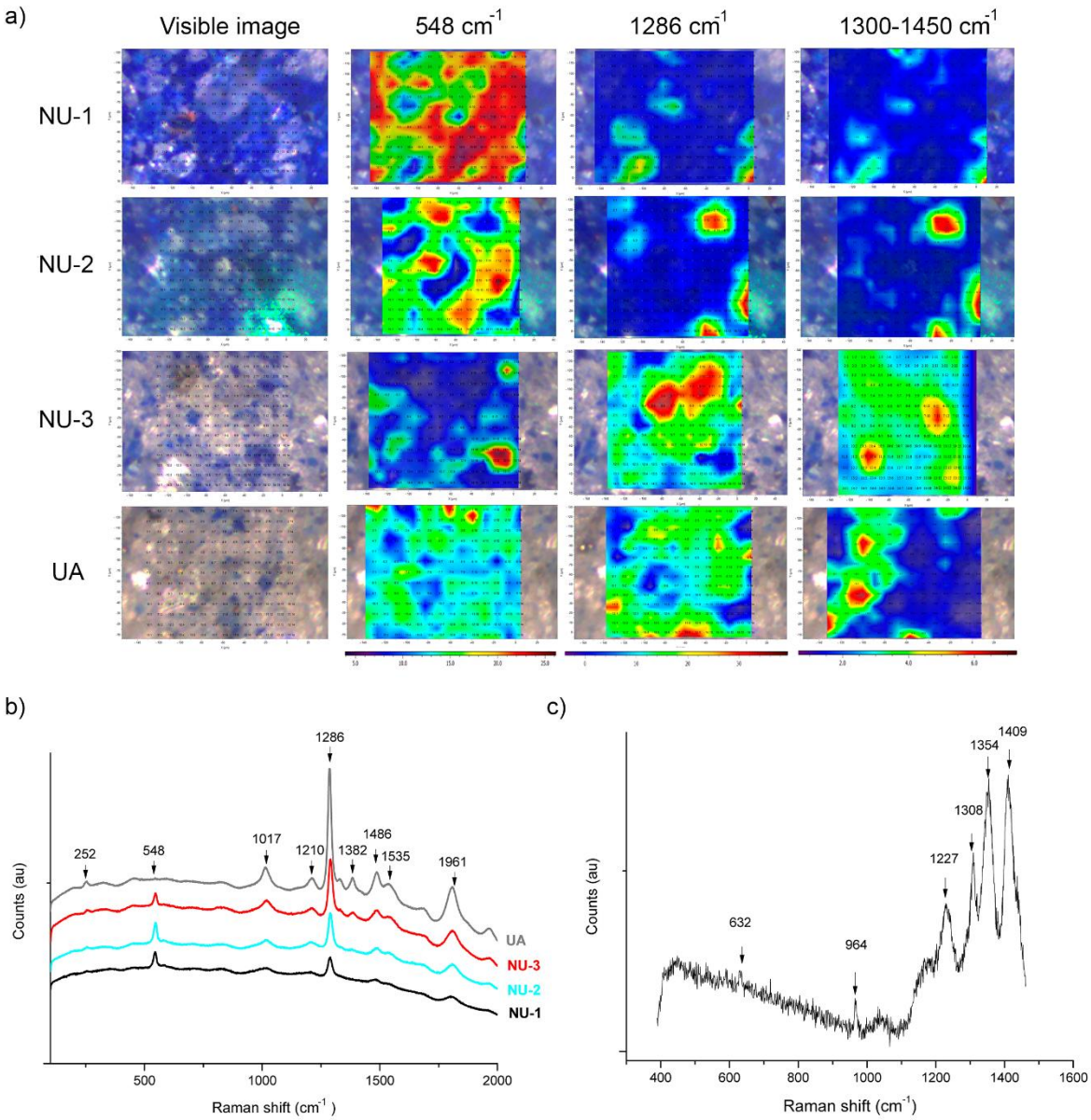

Figure 5. (a) Visible images and distribution maps of the bands at 548 cm^{-1}, 1286 cm^{-1} and the region 1300-1450 cm^{-1}, (b) typical Raman spectra of the pigments with different quality, and (c) Raman

spectrum collected in a peculiar point of the region between 1300-1500 cm^{-1} for the UA sample. Spectra were stacked for better visualization.

In order to better investigate the crystalline phases present in the samples, we performed X-ray diffraction (Figure 6a). As expected, the two synthetic pigments showed very similar diffraction patterns to lazurite as the major crystalline phase identified. This is also the result obtained for the purest natural pigment, NU-1, where again lazurite was undoubtedly identified as the major mineral phase. This is in agreement with previous studies that reported that the first separation step of the traditional purification process extracts lazurite as the dominant phase [44]. Diffraction patterns become much more complex when the quality of the pigments decreases, due to the increase in the content of accessory minerals. Diopside was distinctly identified in all of the natural pigments, with increasing concentration in samples of lower quality, being even the major phase found in the samples NU-2, NU-3 and UA. Other accessory minerals identified were haüyne, sodalite and phlogopite.

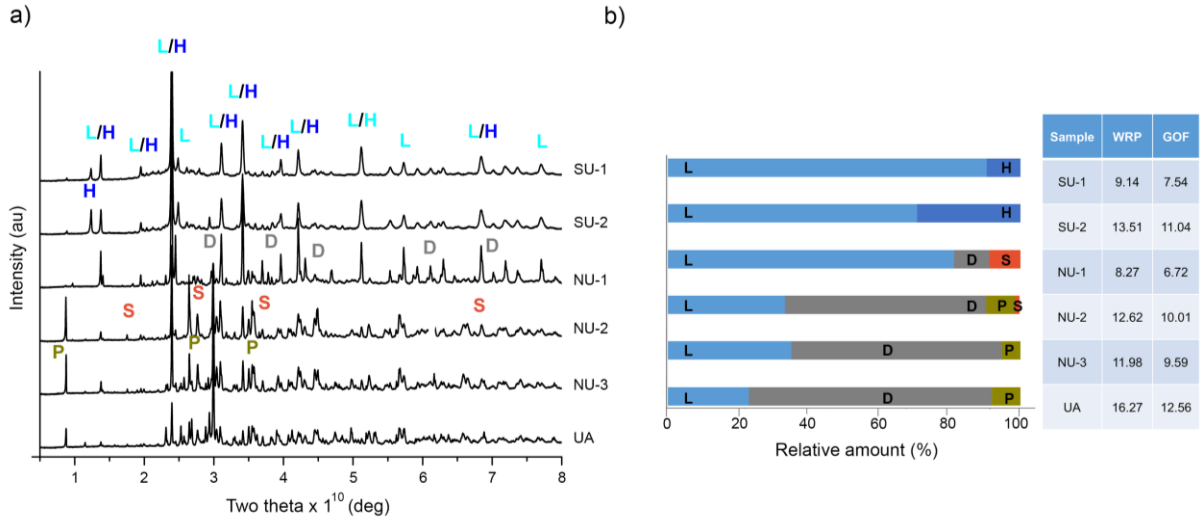

Figure 6. (a) X-Ray diffractograms and (b) Rietveld method quantification results of the different pigment samples. L=Lazurite, H=Haüyne, D=Diopside, P=Phlogopite, S=Sodalite. WRP=weighted residual profile, GOF=goodness of fit. Diffractograms were stacked for better visualization.

Thus, it can be concluded that diopside must be the responsible phase for the luminescence bands found in the Raman spectra in the region around 1286 cm^{-1}. However, we cannot attribute these spectral features to diopside mineral itself since the conventional Raman spectrum of diopside does not show such luminescent features [45]. Such features could be due to impurities and, for this reason, the luminescence emission, although it was clearly associated with colourless areas, it concentrates in certain spots, not being homogenously distributed in all white/grey areas of the samples. Nevertheless, it was not possible to obtain useful Raman signatures in most

white/colourless areas that allow unequivocal identification. In the case of the sample of ultramarine ash (poorest quality, UA) it is noticeable a different spectral pattern, which is present only in certain areas but it is particularly intense (see Figure 5c). In this case, the two weak bands below 1000 cm^{-1} (located at 964 and 632 cm^{-1}) are in good agreement with those reported for wollastonite ($CaSiO_3$) [46]. However, again the broad and strong bands in the region of 1300-1450 cm^{-1} are more likely to be due to luminescence phenomena but, in this case, with a different origin than the pattern described before with the major band at 1286 cm^{-1}. In general, luminescence is caused and influenced by several mechanisms promoting the formation of luminescence centres. The "activators" are mainly chemical impurities in the mineral structure, structural defects and vacancies (non-stoichiometries). Luminescence activators and quenchers for different minerals include rare earth elements, Fe^{2+}, Fe^{3+}, Co^{2+} and Ni^{2+} [47].

Another interesting task is to test the feasibility of performing a quantitative analysis of lazurite content based on Raman images obtained using 785 nm as the excitation source. To do this, an intensity threshold of 1,5 (out of a maximun intensity of 10) was set and black and white maps were built by converting those pixels whose value lie under/above this threshold to to black and white, respectively. This was performed for the band of lazurite (548 cm^{-1}) and for the most intense luminescence band (1286 cm^{-1}). The results are shown in the supplementary information (Figure S1).

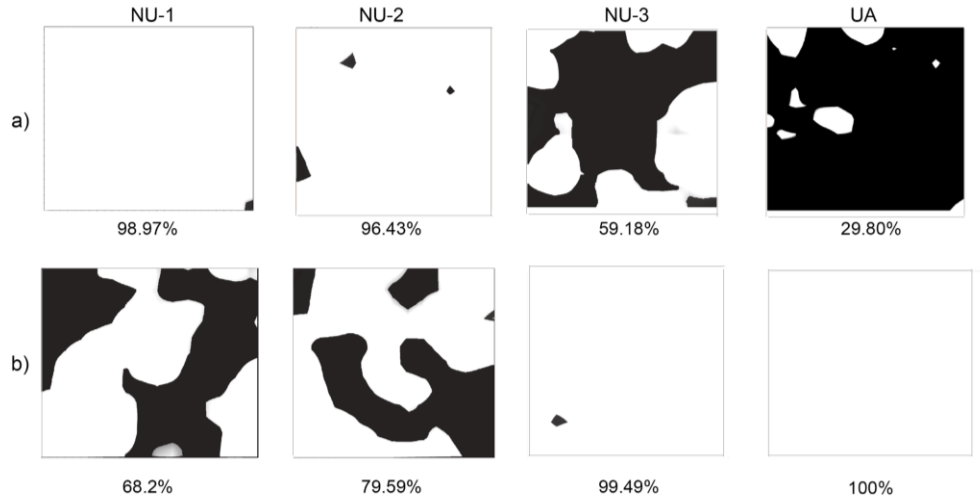

Figure S1. Black and white maps of lapis lazuli samples showing pixels below and above the established threshold, respectively, for (a) 548 cm^{-1} and (b) 1286 cm^{-1} bands. The percentage of pixels above the threshold is given.

As can be seen in Figure 7, there is a good correlation ($R^2 = 0.9057$) between the results for the band at 548 cm^{-1} and the colourimetric parameter b*, which is a measurement of the blue tonality of the samples. A certain relationship ($R^2 = 0.7627$) is also obtained between the percentage of pixels

above the threshold for the luminescence band (1286 cm^{-1}) and the amount of diopside obtained by XRD (Figure 7b), showing that the lower the pigment quality, the greater the diopside mineral content and the higher the intensity of this luminescence band. Although these results are promising, the sample set is very limited and further studies have to be performed to confirm the correlations, especially taking into account the heterogeneity of natural lapis lazuli sources.

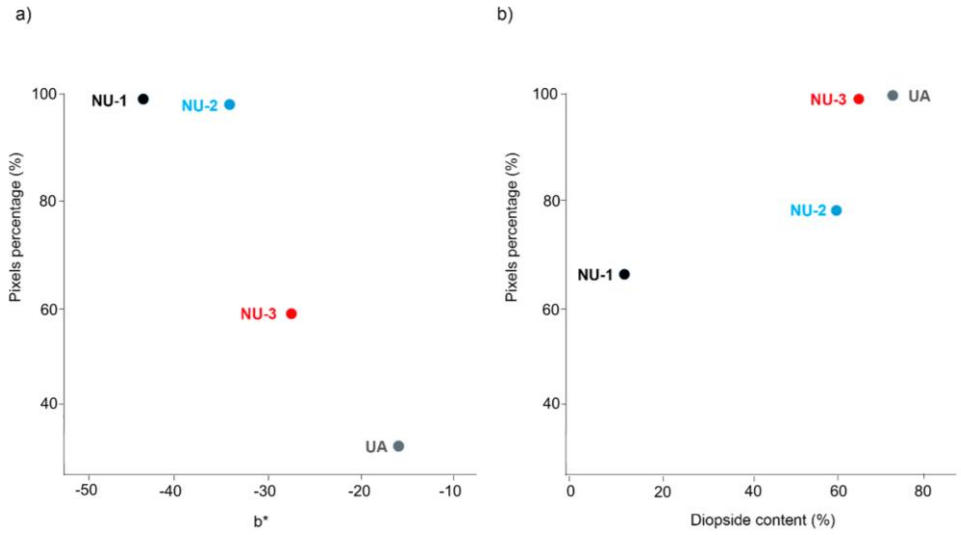

Figure 7. Graphs showing the correlation between the percentage of pixels containing (a) the 548 cm^{-1} band *vs* b* parameter of CIELAB and (b) the 1286 cm^{-1} band *vs* the content (%) of diopside mineral for each sample.

3.3 Application to the investigation of historical decorations

Ultramarine can be found in different decorative revetments of the Alhambra, including polychrome plasterwork in domes, decorated marble capitals and polychrome carpentry. Different decorative motifs showing blue colour (with distinct colour hue) were investigated in order to compare their Raman spectra and identify whether the employed pigment was natural or synthetic. In some cases, there was information from historical sources about the origin of the pigment whereas in other cases not. In Figure 8, a summary of the obtained results from *in situ* measurements is presented, including a representative image of the decorative motifs.

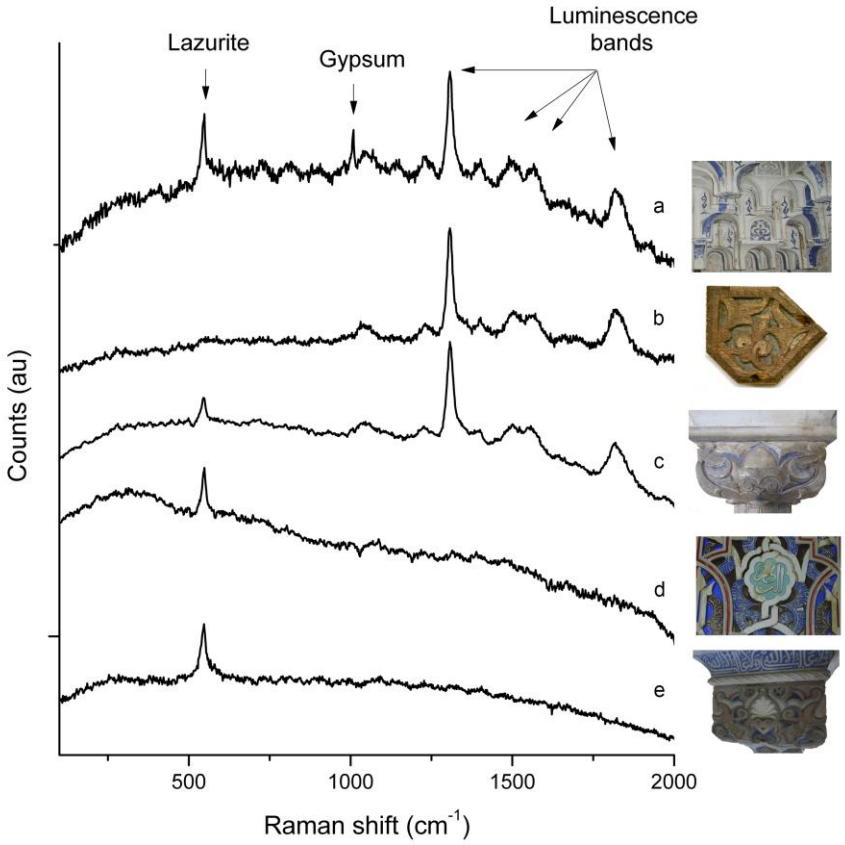

Figure 8. *In situ* Raman spectra registered by using 785 nm laser excitation in different rooms of the Alhambra Monumental Ensemble. Different supports were considered being plasterwork (a, Hall of the Kings, and d, Room of the Beds), wooden ceilings (b, Hall of the Abencerrages) and marble capitals (c and e, Hall of the Mexuar). Spectra were stacked for better visualization and linked to the images of the decorative motifs. Both natural and synthetic ultramarine were found.

The decorations under study were in very different conservation condition. Some motifs showed intense and bright blue colour, whereas in other cases the blue pigment was partially detached or covered with layers of dirt. Raman spectra recorded allowed a straightforward distinction between natural and synthetic ultramarine blue thanks to the luminescence bands in the region 1200-2000 cm^{-1}. Natural ultramarine blue was found in most of the spaces investigated, including plasterwork decorations of the *mocarabes* (stalactites-like) domes of the Hall of the Kings, marble capitals of several courts and halls and the polychrome wooden ceiling of the Hall of the Abencerrages. Differences in the relative intensity of the lazurite/luminescence bands in the spectra of the natural ultramarine blue were also found, that could be related to the quality of the pigments employed. Particularly in the case of the wooden ceiling, the 548 cm^{-1} band is barely recognized, whereas the luminescence bands appearing between 1300-1500 cm^{-1} are very intense. In the case of the marble capitals, even though the luminescence bands are clearly visible, the main band of lazurite appears always with a higher intensity revealing the use of a better quality pigment. The synthetic version

of ultramarine was the only pigment detected in the plasterwork decorations of the Room of the Beds. This finding is in agreement with the historical knowledge about the monument since this Hall was completely redecorated by the architect Rafael Contreras´ in the 19th century [48]. Furthermore, synthetic ultramarine blue was also the pigment employed in the colour reintegration of lost parts carried out in one of the marble capitals of the Hall of the Mexuar at the end of the 20th century.

Although this non-invasive approach is the most adequate for the investigation of historical pigments, we also had the possibility of studying two fragments of plasterwork with blue decoration that were detached during the intervention of the Hall of the Kings. Hyperspectral Raman images were registered with similar measurement conditions to the ones with powder commercial pigments. Results can be observed in Figure 9. The visible images show a very heterogeneous distribution of blue and white areas but in this case, we must take into account the contribution of the gypsum support on which the pigment was applied.

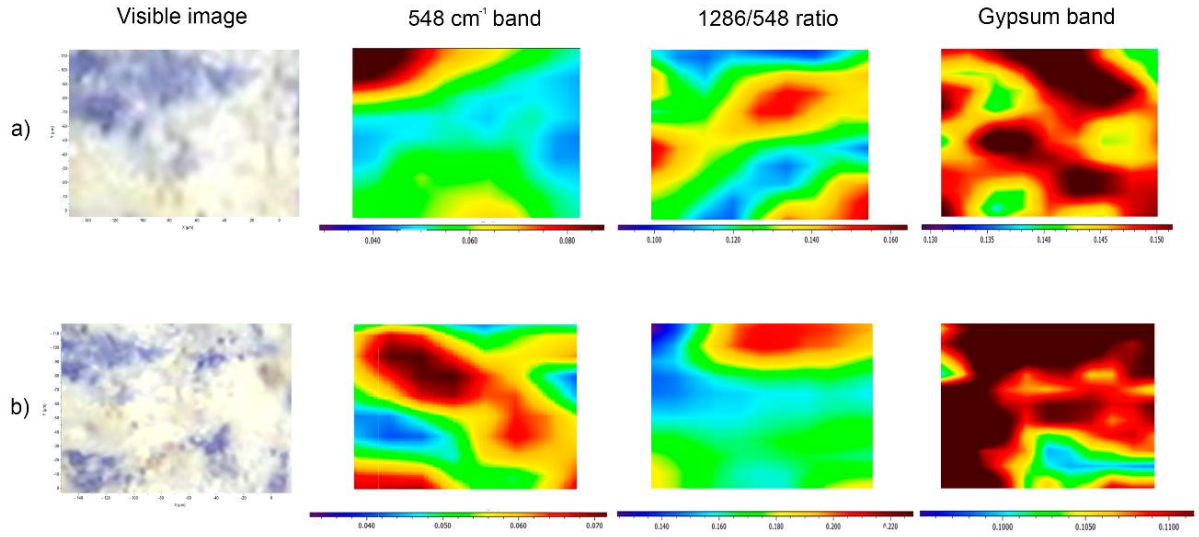

Figure 9. Visible images of the two small historical decorations from vaults (a) 4 and (b) 6 of the Hall of the Kings samples and corresponding distribution maps of 548 cm^{-1} intensity band, the ratio 1286/548 cm^{-1} and the gypsum band (1008 cm^{-1}) recorded with 785 nm laser excitation source.

The analysis in those samples is much more complex than the one with commercial pigments, as the pigment is not homogeneously distributed and white areas can correspond not only to accessory minerals in lapis lazuli but also to gypsum support. In fact, the distribution of the gypsum band (1008 cm^{-1}) is all over the sample image. In order to estimate the quality of the pigment employed in these decorations, we calculated the percentage of pixels above and below the threshold in the

same way than for the commercial pigments. Results for the samples of vault 6 (60.8% and 98.3% for 548 and 1286 cm^{-1}, respectively) were very similar to those obtained for the sample NU-3, which is a medium quality pigment. The much lower percentage of pixels of lazurite band (9.1 %) in the case of the sample from vault 4, does not fit with any of the studied pigments. This can be due to the use of a much lower quality pigment or even the use of ground lapis lazuli without purification. Another possible explanation could be the partial detachment of the lazurite particles while impurities remain in the decoration showing the characteristic luminescence pattern. In any case, it is clear that luminescent impurities can vary a lot in historical samples depending on the sources of natural ultramarine blue and on the employed purification method. Consequently, in order to understand if it would be possible to establish the quality of the natural ultramarine blue as the basis of its luminescent signal, a larger number of historical samples should be considered in future research. This would allow to study and characterize the amounts and types of luminescent impurities that can be present in the different degrees of quality of natural ultramarine blue.

4.- Conclusions

The characteristic pattern of luminescence bands emerging in the zone between 1200-2000 cm^{-1} when 785 nm laser excitation is used to record the Raman spectra of natural ultramarine blue pigments allows a clear differentiation from synthetic ones. This information can be obtained simultaneously with Raman signatures and, when using microscopy, it is useful to extract information about sample heterogeneities in the form of hyperspectral microimages. Spatial distribution of the lazurite characteristic band at 548 cm^{-1} and the luminescence features in natural pigments of different qualities clearly revealed the relationship between the latter and the impurities present in higher proportion in the lowest quality pigments. Furthermore, the luminescence of the number of pixels of selected bands over a certain threshold can be used as a purity criterion and it is also related to colourimetric parameters.

Since natural ultramarine blue pigments were traditionally prepared from finely ground lapis lazuli, their differentiation from synthetic pigments has been mainly based in the detection of analytical signatures of other components of the rock matrix either elements (Ca, Mg and trace elements) or minerals like calcite, diopside, wollastonite, etc. Here, the information obtained by XRF analysis also showed huge differences in the content of some elements, mainly Mg and Ca between natural and synthetic samples. Furthermore, the amount of Ca is significantly increasing as the quality of the natural pigments decreases from the purest one to ultramarine ash. For example, diopside was clearly identified by XRD in natural pigments, However, the analysis of standard pigments is a distant analogy to real samples, and when dealing, for instance, with wall paintings, interferences

from substrate and ground preparation layers typically composed of calcite, gypsum and/or different earth materials, can be important. On the contrary, the luminescent emission observed seems to be unique to minerals accompanying genuine lazurite. Therefore, the proposed approach is able to easily differentiate natural ultramarine blue from synthetic even in presence of complex grounds like those found in the Alhambra monument.

Acknowledgements

Authors would like to acknowledge to FQM-363 Research group, CICT of the Universidad de Jaén and Research project BIA2017-87131-R from the Ministry of Economy and Competitiveness for technical and financial support. M. González-Cabrera and P. Arjonilla also acknowledge the FPU15/03119 (Spanish Ministry of Education, Culture and Sport) and the BES-2014-068793 (Ministry of Economy and Competitiveness) fellowships, respectively. Authors are also grateful to the Council of Alhambra and Generalife for their support. M.T. BRANDAO ESPAÑA S.L is acknowledged for the access to the XploRA Plus Horiba instrument.

References

[1] J. Plesters, Ultramarine Blue, Natural and Artificial, in: Ashok Roy (Ed.), Artist. Pigment. A Handb. Their Hist. Charact., 1993: 1–232.

[2] M.C. Gaetani, U. Santamaria, C. Seccaroni, The Use of Egyptian Blue and Lapis Lazuli in the Middle Ages - The Wall Paintings of the San Saba Church in Rome, Stud. Conserv. 49 (2004) 13–22.

[3] A.A. Finch, H. Friis, M. Maghrabi, Defects in sodalite-group minerals determined from X-ray-induced luminescence, Phys. Chem. Miner. 43 (2016) 481–491.

[4] D. Arieli, A. D. E. W. Vaughan, D. Goldfarb, New Synthesis and Insight into the Structure of Blue Ultramarine Pigments, J. Am. Chem. Soc. 126 (2004) 5776–5788.

[5] I. Hassan, R.C. Peterson, H.D. Grundy, The structure of lazurite, ideally $Na_6Ca_2(Al_6Si_6O_{24})S_2$, a member of the sodalite group, Acta Crystallogr. Sect. C Cryst. Struct. Commun. 41 (1985) 827–832.

[6] P. Ballirano, A. Maras, Mineralogical characterization of the blue pigment of Michelangelo's fresco "The Last Judgment," Am. Mineral. 91 (2006) 997–1005.

[7] D. Reinen, G.-G. Lindner, The nature of the chalcogen colour centres in ultramarine-type solids, Chem. Soc. Rev. 28 (1999) 75–84.

[8] Cennino Cennini, Il libro dell'arte, Le Monnier, 1859.

[9] M. Favaro, A. Guastoni, F. Marini, S. Bianchin, A. Gambirasi, Characterization of lapis lazuli and corresponding purified pigments for a provenance study of ultramarine pigments used in works of art, Anal. Bioanal. Chem. 402 (2012) 2195–2208.

[10] C.M. Schmidt, M.S. Walton, K. Trentelman, Characterization of Lapis Lazuli Pigments Using a Multitechnique Analytical Approach: Implications for Identification and Geological Provenancing, Anal. Chem. 81 (2009) 8513–8518.

[11] A. Re, A. Lo Giudice, D. Angelici, S. Calusi, L. Giuntini, M. Massi, G. Pratesi, Lapis lazuli provenance study by means of micro-PIXE, Nucl. Instruments Methods Phys. Res. Sect. B Beam Interact. with Mater. Atoms. 269 (2011) 2373–2377.

[12] A. Banerjee, T. Häger, On some Crystals of "Lapis Lazuli," Zeitschrift Fur Naturforsch. - Sect. A J. Phys. Sci. 47 (1992) 1094–1095.

[13] I. Osticioli, N.F.C. Mendes, A. Nevin, F.P.S.C. Gil, M. Becucci, E. Castellucci, Analysis of natural and artificial ultramarine blue pigments using laser induced breakdown and pulsed Raman spectroscopy, statistical analysis and light microscopy, Spectrochim. Acta Part A Mol. Biomol. Spectrosc. 73 (2009) 525–531.

[14] R. Nečas, D. Všianský, Ultramarine – Not Just a Pigment of Traditional Folk Architecture Plasters, Procedia Eng. 151 (2016) 114–118.

[15] E. Climent-Pascual, R. Sáez-Puche, A. Gómez-Herrero, J.R. de Paz, Cluster ordering in synthetic ultramarine pigments, Microporous Mesoporous Mater. 116 (2008) 344–351.

[16] C.E. Silva, L.P. Silva, H.G.M. Edwards, L.F.C. de Oliveira, Diffuse reflection FTIR spectral database of dyes and pigments, Anal. Bioanal. Chem. 386 (2006) 2183–2191.

[17] Q.G. Zeng, G.X. Zhang, C.W. Leung, J. Zuo, Studies of wall painting fragments from Kaiping Diaolou by SEM/EDX, micro Raman and FT-IR spectroscopy, Microchem. J. 96 (2010) 330–336.

[18] C. Miliani, A. Daveri, B.G. Brunetti, A. Sgamellotti, CO_2 entrapment in natural ultramarine blue, Chem. Phys. Lett. 466 (2008) 148–151.

[19] M.R. Derrick, J.M. Landry, Scientific Tools for Conservation Infrared Spectroscopy in Conservation Science, Los Angeles, 1999.

[20] G.D. Smith, R.J. Klinshaw, The presence of trapped carbon dioxide in lapis lazuli and its potential use in geo-sourcing natural ultramarine pigment, J. Cult. Herit. 10 (2009) 415–421.

[21] M. Aceto, A. Agostino, G. Fenoglio, M. Picollo, Non-invasive differentiation between natural and synthetic ultramarine blue pigments by means of 250–900 nm FORS analysis, Anal. Methods. 5 (2013) 4184–4189.

[22] A.R. De Torres, S. Ruiz-Moreno, A. López-Gil, P. Ferrer, M.C. Chillón, Differentiation with Raman spectroscopy among several natural ultramarine blues and the synthetic ultramarine blue used by the Catalonian modernist painter Ramon Casas i Carbó, J. Raman Spectrosc. 45 (2014) 1279–1284.

[23] R. Salzer, H.W. Siesler, eds., Infrared and Raman Spectroscopic Imaging, Wiley-VCH Verlag GmbH & Co. KGaA, Weinheim, Germany, 2009.

[24] H.F. Grahn, P. Geladi, Techniques and Applications of Hyperspectral Image Analysis, J. Wiley, 2007.

[25] P. Arjonilla, A. Domínguez-Vidal, M.J. de la Torre López, R. Rubio-Domene, M.J. Ayora-Cañada, In situ Raman spectroscopic study of marble capitals in the Alhambra monumental ensemble, Appl. Phys. A. 122 (2016) 1014.

[26] A. Dominguez-Vidal, M. Jose De La Torre-Lopez, R. Rubio-Domene, M.J. Ayora-Cañada, In situ noninvasive Raman microspectroscopic investigation of polychrome plasterworks in the Alhambra, Analyst. 137 (2012) 5763–5769.

[27] P. Arjonilla, M.J. Ayora-Cañada, R. Rubio Domene, E. Correa Gómez, M.J. de la Torre-López, A. Domínguez-Vidal, Romantic restorations in the Alhambra monument: Spectroscopic characterization of decorative plasterwork in the Royal Baths of Comares, J. Raman Spectrosc. 50 (2019) 184–192.

[28] P. Arjonilla, A. Domínguez-Vidal, E. Correa-Gómez, M.J. Domene-Ruiz, M.J. Ayora-Cañada, Raman and Fourier transform infrared microspectroscopies reveal medieval Hispano–Muslim wood painting techniques and provide new insights into red lead production technology, J. Raman Spectrosc. 50 (2019) 1537–1545.

[29] P. Arjonilla, A. Domínguez-Vidal, E. Correa-Gómez, R. Rubio-Domene, A. Lluveras-Tenorio, M.J. Ayora-Cañada, M.P. Colombini, Characterization of organic materials in the decoration of ornamental structures in the Alhambra monumental ensemble using gas-chromatography/mass spectrometry (GC/MS), Microchem. J. 140 (2018) 14–23.

[30] A. Dominguez-Vidal, M.J. De La Torre-López, M.J. Campos-Suñol, R. Rubio-Domene, M.J. Ayora-Cañada, Decorated plasterwork in the Alhambra investigated by Raman spectroscopy:

Comparative field and laboratory study, J. Raman Spectrosc. 45 (2014) 1006–1012.

[31] C. Cardell, L. Rodriguez-Simon, I. Guerra, A. Sanchez-Navas, Analysis of Nasrid polychrome carpentry at the Hall of the Mexuar Palace, Alhambra complex (Granada, Spain), combining microscopic, chromatographic and spectroscopic methods, Archaeometry. 51 (2009) 637–657.

[32] Hunter Lab, CIE L*a*b* Color Scale. Insight on color, Apl. Note. 8 (1996).

[33] M. Etter, R.E. Dinnebier, A Century of Powder Diffraction: a Brief History, Zeitschrift Für Anorg. Und Allg. Chemie. 640 (2014) 3015–3028.

[34] D. Reinen, G.-G. Lindner, The nature of the chalcogen colour centres in ultramarine-type solids, Chem. Soc. Rev. 28 (1999) 75–84. d

[35] R.J.H. Clark, T.J. Dines, M. Kurmoo, On the nature of the sulfur chromophores in ultramarine blue, green, violet, and pink and of the selenium chromophore in ultramarine selenium: characterization of radical anions by electronic and resonance Raman spectroscopy and the determination of their excited-state geometries, Inorg. Chem. 22 (1983) 2766–2772.

[36] M. Bacci, C. Cucci, E. Del Federico, A. Ienco, A. Jerschow, J.M. Newman, M. Picollo, An integrated spectroscopic approach for the identification of what distinguishes Afghan lapis lazuli from others, Vib. Spectrosc. 49 (2009) 80–83.

[37] L. Goncalves, D. Moronta, F. Ocanto, C. Linares, Synthesis of ultramarine blue type pigments using several raw materials, Rev. La Fac. Ing. Univ. Cent. Venez. 25 (1986) 25–31.

[38] S. Kowalak, M. Pawłowska, M. Miluśka, M. Stróżyk, J. Kania, W. Przystajko, Synthesis of ultramarine from synthetic molecular sieves, Colloids Surfaces A Physicochem. Eng. Asp. 101 (1995) 179–185.

[39] R.J.H. Clark, M.L. Curri, C. Laganara, Raman microscopy: The identification of lapis lazuli on medieval pottery fragments from the south of Italy, Spectrochim. Acta Part A Mol. Biomol. Spectrosc. 53 (1997) 597–603.

[40] P. Colomban, A. Tournié, M.C. Caggiani, C. Paris, Pigments and enamelling/gilding technology of Mamluk mosque lamps and bottle, J. Raman Spectrosc. 43 (2012) 1975–1984.

[41] O. El Jaroudi, E. Picquenard, A. Demortier, J.P. Lelieur, J. Corset, Polysulfide anions II: Structure and vibrational spectra of the S_4^{2-} and S_5^{2-} anions. Influence of the cations on bond

length, valence, and torsion angle, Inorg. Chem. 39 (2000) 2593–2603.

[42] R.R. Hark, R.J.H. Clark, P.M. Champion, L.D. Ziegler, Raman Microscopy of Diverse Samples of Lapis Lazuli at Multiple Excitation Wavelengths, AIP Conf. Proc. 1267 (2010) 315–316.

[43] E.M.A. Ali, H.G.M. Edwards, Analytical Raman spectroscopy in a forensic art context: the non-destructive discrimination of genuine and fake lapis lazuli., Spectrochim. Acta. A. Mol. Biomol. Spectrosc. 121 (2014) 415–419.

[44] M. Favaro, A. Guastoni, F. Marini, S. Bianchin, A. Gambirasi, Characterization of lapis lazuli and corresponding purified pigments for a provenance study of ultramarine pigments used in works of art, Anal. Bioanal. Chem. 402 (2012) 2195–2208.

[45] M. Prencipe, L. Mantovani, M. Tribaudino, D. Bersani, P.P. Lottici, The Raman spectrum of diopside: a comparison between ab initio calculated and experimentally measured frequencies, Eur. J. Miner. 24 (2012) 457–464.

[46] G.C. Serghiou, W.S. Hammack, Pressure-induced amorphization of wollastonite ($CaSiO_3$) at room temperature, J. Chem. Phys. 98 (1993) 9830–9834.

[47] A.S. Marfunin, Spectroscopy, Luminescence and Radiation Centers in Minerals, Springer Berlin Heidelberg, Berlin, Heidelberg, 1979.

[48] A. González Pérez, Reconstructing the Alhambra: Rafael Contreras and Architectural Models of the Alhambra in the Nineteenth Century, Art Transl. 9 (2017) 29–49.